JOURNAL OF GEOPHYSICAL RESEARCH, VOL. 115, G01009, doi:10.1029/2008JG000906, 2010



# Soil $CO_2$ production in upland tundra where permafrost is thawing

Hanna Lee,[1,2] Edward A. G. Schuur,[1] and Jason G. Vogel[3]

Received 5 December 2008; revised 12 September 2009; accepted 25 September 2009; published 16 February 2010.

[1] Permafrost soils store nearly half of global soil carbon (C), and therefore permafrost thawing could lead to large amounts of greenhouse gas emissions via decomposition of soil organic matter. When ice-rich permafrost thaws, it creates a localized surface subsidence called thermokarst terrain, which changes the soil microenvironment. We used soil profile $CO_2$ measurements to understand the response of belowground C emissions for different soil depths from upland tundra as a result of permafrost thaw and thermokarst development. We established sites in central Alaska, where permafrost thaw and thermokarst development had been monitored for the past 2 decades. Cumulative growing season $CO_2$ production averaged for 3 years (2005–2007) ranged from 177 to 270 g $CO_2$-C $m^{-2}$ and was lowest in the least disturbed moist acidic tundra and highest where thawing of permafrost and thermokarst was most pronounced. We were able to explain 55% of variability in growing season soil $CO_2$ production using surface subsidence, soil temperature, and site differences. This was likely a direct effect of permafrost thaw and thermokarst development and an indirect effect of changes in microsite soil temperature and surface moisture content, which stimulated soil organic matter decomposition and root respiration. We also observed unusually high $CO_2$ concentrations in the early growing season, which may be attributable to trapped $CO_2$ within air pockets in the frozen soil. Taken together, these results supported the projection that permafrost thaw and thermokarst development will increase belowground carbon emissions in the upland tundra.

**Citation:** Lee, H., E. A. G. Schuur, and J. G. Vogel (2010), Soil $CO_2$ production in upland tundra where permafrost is thawing, *J. Geophys. Res.*, *115*, G01009, doi:10.1029/2008JG000906.

## 1. Introduction

[2] Over the past century, high-latitude ecosystems have undergone drastic changes due to global-scale warming [*Arctic Climate Impact Assessment* (*ACIA*), 2005; *Serreze et al.*, 2000]. One consequence of warming in high-latitude ecosystems is permafrost thaw. Permafrost soil is distributed across 14% of the global land surface [*Tarnocai et al.*, 2009], and accounts for more than half of global terrestrial soil carbon (C) [*Schuur et al.*, 2008]. Recent studies have shown increased permafrost temperatures as deep as 50 m [*Osterkamp and Romanovsky*, 1999] due to increased mean annual temperature and changes in precipitation. This may expose soil organic matter stored in permafrost to microbial decomposition, releasing greenhouse gases such as carbon dioxide ($CO_2$) at a faster rate. These emissions may create a positive feedback cycle between global warming and permafrost thaw.

[3] When ice-rich permafrost thaws, it may create a ground surface subsidence called thermokarst terrain. Thermokarst terrains may alter the soil environment by changing soil hydrology, which in turn contributes to changes in microsite soil temperature, moisture, and nutrient availability [*Fortier et al.*, 2007; *Jorgenson et al.*, 2001; *Osterkamp*, 2007b]. A subsided ground surface increase active layer thickness (ALT), the seasonally thawed soil layer found in the permafrost zone, and expose deeper permafrost to further thaw, which in turn may stimulate decomposition of soil organic matter stored deep within.

[4] Several studies have observed increased ecosystem C emissions from climatic changes in high-latitude ecosystems [*Oechel et al.*, 2000; *Shaver et al.*, 1998; *Vourlitis and Oechel*, 1999; *Welker et al.*, 2000]. However, chamber flux measurements and eddy covariance methods of measuring $CO_2$ exchange cannot distinguish between belowground and aboveground C emissions. Some researchers have observed belowground $CO_2$ emissions directly by detecting $CO_2$ gas from different soil profiles using gas wells or other similar instruments [*Davidson and Trumbore*, 1995; *Elberling and Ladegaard-Pedersen*, 2005; *Hirsch et al.*, 2002; *Oh et al.*, 2005; *Risk et al.*, 2002; *Takahashi et al.*, 2004; *Tang et al.*, 2003]. Using Fick's law of gaseous diffusion, observations of soil $CO_2$ concentration in a soil profile can be used to quantify $CO_2$ production from individual soil layers and to estimate total belowground $CO_2$ production as soil $CO_2$ production [*Davidson and Trumbore*, 1995].

[1]Department of Biology, University of Florida, Gainesville, Florida, USA.
[2]Now at Department of Biology, New Mexico State University, Las Cruces, New Mexico, USA.
[3]School of Forest Resources and Conservation, University of Florida, Gainesville, Florida, USA.


0148-0227/10/2008JG000906$09.00

[5] In this study, we estimated soil $CO_2$ production from a natural permafrost thaw gradient to examine how permafrost thaw and thermokarst development over decadal timescales affects $CO_2$ emissions from an upland tundra ecosystem. We hypothesized that soil $CO_2$ production would increase with the degree of permafrost thaw and thermokarst development especially in the deeper soil layers, because increased soil temperature and moisture would stimulate root respiration and microbial decomposition of soil organic matter.

## 2. Site Description

[6] This study was conducted in upland tundra near Healy, Alaska, just outside of Denali National Park (Eight Mile Lake gradient site: 63°52′42″N, 149°15′12″W). At this site, ground temperature and deep permafrost temperatures to depths of 30 m have been monitored since 1985 [*Osterkamp and Romanovsky*, 1999]. Ground subsidence as a result of permafrost thaw and thermokarst has also been observed within the landscape [*Osterkamp*, 2005]. The area is a gentle north facing slope (<5°) with discharge water draining into the adjacent Eight Mile Lake. The organic horizon, 0.45–0.65 m thick, covers cryoturbated mineral soil that is a mixture of glacial till (small stones and cobbles) and windblown loess. Permafrost was found within one meter of the soil surface, classifying these soils in the order Gelisol. Three sites were established in 2003 based on the degree of permafrost thaw and resulting ground subsidence [*Schuur et al.*, 2007]: Minimal Thaw is the least disturbed typical moist acidic tussock tundra site scarcely covered by dwarf shrub sublayer dominated by tussock forming sedges (*Eriophorum vaginatun* and *Carex spp.*) and an understory of mosses and lichens, with little ground subsidence. Moderate Thaw is located adjacent to the permafrost monitoring borehole [*Osterkamp and Romanovsky*, 1999], where patchy areas of ground subsidence have started to occur. The vegetation composition of Moderate Thaw was similar to Minimal Thaw, but with increased biomass of all plant groups. Extensive Thaw contains large-scale ground subsidence and shrubs such as blueberry (*Vaccinium uliginosum*) and cloudberry (*Rubus chamaemorus*), that have become the dominant vegetation at the expense of tussock-forming sedges [*Schuur et al.*, 2007].

[7] Soil organic pools to a depth of 1 m averaged 59.8 ± 2.8 kg C $m^{-2}$ across all three sites. The ratio of carbon to nitrogen (C:N) in surface 5–15 cm soils ranged from 33.4 to 57.6 across all three sites, but the C:N at the three sites were not statistically different (H. Lee, unpublished data, 2009). The mean active layer measured from 2004 to 2006 at the Extensive Thaw site (78.3 ± 4.5 cm) was greater than that of the Minimal Thaw (68.7 ± 2.0 cm), with Moderate Thaw (70.0 ± 2.0 cm) being the intermediate, but not significantly different from the other sites [*Vogel et al.*, 2009]. The changes in ground topography as a result of subsidence has resulted in a complex microtopography, where subsided areas collect water and become water saturated, while nearby relatively elevated areas become drier within the same site [*Lee et al.*, 2007]. These different moisture conditions are coupled with soil temperature, microsite differences in plant community composition, and increased active layer thickness (ALT), with more saturated areas having deeper thaw depth.

## 3. Materials and Methods

### 3.1. Gas Well Measurements

[8] We used soil gas wells to collect gas from the soil profile in order to estimate $CO_2$ production from different soil layers. Gas wells were constructed from 1/8″ diameter stainless steel tubing. The tubing had the length of the designated depth (10, 20, 30, and 40 cm) plus an additional 30 cm for the aboveground and an additional 30 cm, which was bent into an L shape and pushed horizontally into the face of the soil profile at designated depths within the soil profile. At the soil surface, an airtight stopcock was glued to the end of the stainless steel tubing and was kept closed, except during sampling to minimize ambient air exchange with soil gas. Gas wells had three holes near the tip that went in to the soil profile, which was wrapped around with mesh cloth to decrease the chance of clogging by soil organic matter or silt. Five gas well locations were established at each site in 2004, with each location having wells at four depths in the soil profile (10, 20, 30, and 40 cm). In 2005, we installed gas wells at 6 additional locations at each site, with each site having shorter depth intervals (5, 10, 15, 20, 25, and 30 cm) to obtain finer-scale estimates of soil profile $CO_2$ flux. These gas wells were left in place during the 3 years of study to minimize the disturbance created by installation of the gas wells.

[9] We used airtight plastic syringes to sample 20 mL of gas from each gas well. The gas wells were not purged before sampling, but we assumed that the $CO_2$ concentration inside the tube was same as the $CO_2$ concentrations in the soil layer because it was kept closed. The gas samples were analyzed using an injection valve and loop (Valco Instrumental Company Inc., Houston, TX, Valco 6-port injection valve, 1 mL injection loop) attached to an infrared gas analyzer (Li-820, LI-COR Biosciences, Lincoln, Nebraska). The injection loop attached to the infrared gas analyzer was a closed system that used a preexisting gas scrubbed through a 1 L jar of soda lime. The loop trapped 1 mL of the injected sample, which was later mixed with larger volume of $CO_2$-free air and circulated through an infrared gas analyzer. We used 1,000, 10,000, and 25,000 ppm certified $CO_2$-in-air standards to generate standard curves for the samples measured with the infrared gas analyzer through the injection loop.

[10] Samples were taken weekly throughout the growing season (May–September) from 2005 to 2007 on calm mornings, to minimize pressure-driven soil gas exchange between ambient air and soil that occurs as a result of wind [*Hirsch et al.*, 2004]. We were able to sample $CO_2$ from deeper soil layers in the beginning of the growing season, which was taken from air pockets within frozen soil. These air pockets trapped $CO_2$ during soil surface freeze in the fall and $CO_2$ produced over the winter, which often contained high $CO_2$ concentrations up to 10%. However, since these air pockets were not subject to the standard assumptions of the normal diffusion law, we did not include these measurements in the growing season soil $CO_2$ flux estimates.

[11] On average, across years and sites, we were able to sample gas from ice-free soil starting at day of year 150 for

the 10 cm depth, starting at day of year 165 for the 20 cm depth, and starting at day of year 185 for the 30 cm depth, as the seasonal thaw front descended within the active layer. At the EML gradient sites, deeper soil layers were saturated with water most of the time due to a water table that was perched on the ground ice surface. During rain events, even surface layers (10 cm) could become saturated with water. When soils were waterlogged, we collected 10 mL of soil water and mixed it with 10 mL of ambient air, shook it for 1 min to equilibrate, then measured $CO_2$ from the headspace of the mixed gas sample.

### 3.2. Soil Properties

[12] Soil temperature was measured as the spatial variability of soil temperature instead of a constant monitoring. IButton Thermochron temperature loggers (Maxim Inc., Dallas, TX) were buried adjacent to each gas well at a depth of 10 cm and data-logged for 3 days in continuous 30 min intervals. Mean soil temperatures at 10 cm depths were obtained for the 3 days of measurement and they were normalized to a mean of 0°C. As a result, higher soil temperature estimated from this normalization implies that the gas well was placed at a microsite where soil temperature was higher than average. These were used to describe the spatial variability of soil temperature at each gas well, referred to as soil temperature throughout this study. ALT was measured at the end of the growing season in 2007 adjacent to each gas well by pushing a thin stainless steel rod into the ground until it hit the permafrost surface. The depth to permafrost from the surface was recorded as ALT. Soil moisture content was measured at a location close to gas wells during each gas sampling period in 2006 and 2007. We measured soil moisture as volumetric water content (VWC) using a water content reflectometer (CS616, Campbell Scientific Inc.) and a CR10X data logger. The CS616 was calibrated for the EML gradient sites by comparing CS616 values measured at nearby points to direct water content measurements that were determined through destructive soil sampling from samples taken at the same nearby points. To calibrate the CS616, we vertically installed the probe at 10, 20, and 30 cm depths in the soil at 60 random locations at the EML gradient sites and obtained measurements. Directly afterward, a 10 cm diameter soil core was removed at each location. Soil cores were weighed wet, then dried at 60°C, and reweighed to obtain VWC of the soil. We used linear regressions for each depth to obtain the best fit between CS616 values and direct measure of VWC. We used measurements taken at 10 cm for soil temperature and moisture for further statistical analyses. We measured soil temperatures at 0, 10, 20, 30, and 40 cm at Moderate Thaw, but were not able to monitor soil temperatures at all 33 gas wells. The PCA of soil temperatures at various depths showed that soil temperature at 10 cm best represented the trend in soil temperatures and was the most correlated to soil $CO_2$ production. Also, soil $CO_2$ production was largely driven by production in the surface layer. Therefore, we used measurements taken at 10 cm for spatial variability of soil temperature and soil moisture as explanatory variables to explain growing season soil $CO_2$ production. Mean growing season soil temperature at 10 cm used in Figure 4b was taken from *Vogel et al.* [2009] and J. G. Vogel (unpublished data, 2009), which was measured using a handheld temperature logger attached to thermocouple at the three sites from 2005 to 2007 daily. These measurements were then modeled to generate monthly mean temperature.

### 3.3. Estimating Soil Profile $CO_2$ Flux and Production

[13] We calculated soil profile $CO_2$ flux using Fick's first law from one-dimensional measurements of $CO_2$ concentration at each soil profile.

$$CO_2\,\text{Flux} = -D_{\text{eff}}\, dC/dz \tag{1}$$

[14] In this equation, $D_{\text{eff}}$ is gas diffusion coefficient in soil, $dC$ is the difference of $CO_2$ concentrations between two adjacent soil horizons, and $dz$ is thickness of each soil horizon that was sampled.

[15] The gas diffusion coefficient ($D_{\text{eff}}$) was estimated based on air-filled porosity in soil using Millington's equation, as well as the $CO_2$ gradient [*Davidson and Trumbore*, 1995; *Gaudinski et al.*, 2000; *Hirsch et al.*, 2002; *Millington*, 1959].

$$D_{\text{eff}} = D_0\, e^{4/3}\, (e/a)^2\, (T/273)^{1.75} \tag{2}$$

[16] Here, $D_0$ is diffusivity in air, a is total porosity (1 − Bulk density/Particle density), and e is air-filled porosity (Total porosity − VWC). The diffusion coefficient for $CO_2$ in free air was $1.39 \times 10^{-5}$ $m^2$ $s^{-1}$ [*Gaudinski et al.*, 2000], and $1.7 \times 10^{-9}$ $m^2$ $s^{-1}$ in water [*Jahne et al.*, 1987]. Some estimations of the diffusion coefficient showed lower values than the diffusion coefficient in water, but we assumed that the diffusion coefficient was the same as that in water in those cases. The diffusion coefficient for 2006 and 2007 were estimated for each sampling time period. However, because we did not measure VWC in 2005, we used a mean diffusion coefficient estimated from 2006 and 2007 at each gas well.

[17] Soil profile $CO_2$ flux was estimated from the difference between $CO_2$ concentrations at two different soil depths and the diffusion coefficient (equation (1)). The $CO_2$ production for each layer was calculated as the difference between $CO_2$ fluxes at two adjacent layers (equation (3)).

$$CO_2\,\text{production} = F_i - F_{i+1} \tag{3}$$

where $F_i$ is $CO_2$ flux for one horizon and $F_{i+1}$ is $CO_2$ flux in the horizon below. Soil $CO_2$ production was estimated as a sum of $CO_2$ production for each soil layer across the entire soil profile. Soil $CO_2$ production is sum of root respiration and microbial decomposition of soil organic matter. However, soil $CO_2$ production should be distinguished from surface fluxes or aboveground $CO_2$ production especially in tundra ecosystem, because surface fluxes includes the contribution of aboveground plant respiration.

[18] Soil $CO_2$ production is driven by two major factors: changes in diffusivity and changes in the rate of belowground respiration. The major objective of our study was to observe changes in the rate of belowground respiration as a function of permafrost thaw and thermokarst development. Accurately estimating diffusion coefficient was one of the

most difficult steps in estimating soil $CO_2$ production. The physical characteristic that changes diffusion coefficient the most was VWC in tundra soils; unfortunately we were not able to measure VWC in 2005. Therefore, we compared soil $CO_2$ production estimates in two ways: using unique diffusion coefficients for each gas well at the time of measurement and using a constant diffusion coefficient for each depth interval (0–10, 10–20, and 20–30 cm) across the three sites. In this way, we were able to identify whether changes in soil $CO_2$ production were a result of changes in diffusivity or belowground respiration. Mean soil $CO_2$ production of the two estimates showed the same trend for the three sites, meaning that the changes in soil $CO_2$ production at the EML gradient sites were a result of increased root respiration and microbial decomposition of soil organic matter.

### 3.4. Surface Microtopography

[19] We used a differential Global Positioning System (GPS) [*Little et al.*, 2003] to determine the fine-scale (1 cm vertical resolution) topographical features of all gas well locations and the degree of surface subsidence created by permafrost thaw and thermokarst. We installed one GPS antenna (Trimble 5400) at a nearby USGS marker (WGS84, 63°53′16.56″N, 149°14′17.92″W) and used another GPS antenna to survey gas well coordinates, so that sampling coordinates were always corrected relative to the marker to obtain better accuracy. The x, y, z (longitude, latitude, altitude) coordinates were then normalized for hillslope trends along the z axis to minimize the effect of hillslope. From this, we excluded the top 5% of the z axis measurements as outliers and obtained means of the remaining highest 10% of the points per site. All of the z axis values were normalized according to the mean of the highest 10% of the values as a measure of surface subsidence, which isolated microtopography as a result of thermokarst. This procedure was done separately for each site. Therefore, the surfaces with lower relative elevation largely represent surface subsidence created by permafrost thaw and thermokarst, whereas the surfaces with higher relative elevation represent elevated surfaces that did not subside [*Lee et al.*, 2007]. We used this normalized relative elevation measurement as "Microtopography" throughout this study.

### 3.5. Statistical Analysis

[20] Soil $CO_2$ production data were log transformed to achieve normal distribution of the data to meet the assumptions of regression analysis. We used repeated measures analysis to compare soil $CO_2$ production at each site over multiple time periods. Using Mixed Model in SAS (PROC MIXED statement), sites were fixed with individual wells nested within. We compared "site," "year," and a "site × year" interaction. We used simple regression analysis to model mean growing season soil $CO_2$ production using measured soil variables: spatial variability of soil temperature at 10 cm (T), soil moisture at 10 cm (VWC), ALT, and surface subsidence created by permafrost thaw and thermokarst (Microtopography). We also used the three sites as dummy variables with a slope of 0. Dummy variables indicated the different sites (Site 1 and Site 2), and possibly adjust for the unexplained differences in the sites. The statistical analyses were conducted using SAS 9.0 (SAS Institute Inc., 2002) and JMP 7.0.2 (SAS Institute Inc., 2007).

## 4. Results

### 4.1. Soil Profile $CO_2$ Concentration

[21] Mean $CO_2$ concentrations at different depths in the soil profile ranged from 680 ppmv near the surface to 13,000 ppmv at deeper depths, with the median values ranging from 640 to 5,400 ppmv (Figure 1a). Soil $CO_2$ concentrations varied by site, well, time of the growing season, and with temperature, and precipitation. At every depth profile and year sampled, the mean $CO_2$ concentration was higher than the median, illustrating the influence of some very high $CO_2$ concentrations observed on the mean $CO_2$ concentration. The coefficient of variance for all concentrations was low (CV < 1) for the 5 and 10 cm depths and was higher (CV > 1) for all deeper depths. At this study area, $CO_2$ concentrations increased with depth down to 30 cm, but decreased below 30 cm, possibly due to the presence of permafrost and waterlogged conditions. Generally, the seasonal trend in $CO_2$ concentrations between day of the year 150 and 260 was for the peak values to occur in July (Figure 1b), which follows the trend of seasonal increase in soil temperature and plant productivity during the growing season. However, much higher $CO_2$ concentrations, as high as 1% $CO_2$, were observed even in surface soil layers in the beginning of the growing season (day of year < 150) in 2006 and 2007.

### 4.2. Volumetric Water Content and Soil Gas Diffusion Coefficient

[22] VWC at 10 cm ranged from 0.1 to 0.3 mL $cm^{-3}$, whereas at 30 cm it remained close to 1.0 mL $cm^{-3}$ throughout the growing season as a result of water saturation (Figure 2). In contrast, VWC at 20 cm showed large variation between 0.1 to 1.0 mL $cm^{-3}$ depending on the timing of rainfall events and/or the microtopographical location of individual wells, whether they were located in lower (saturated) or higher (drier) areas. The diffusion coefficient showed an opposite trend from VWC by definition (equation (2)), because air-filled porosity decreases as VWC increases and water slows $CO_2$ diffusion rates. The estimates of the diffusion coefficient indicated that at 30 cm and deeper, the diffusion coefficient was generally the same as that in water, and this corresponded to the fact that a water table was perched on the ice surface throughout the growing season. The ratio of an estimated diffusion coefficient in soil at 10 cm and that of the atmosphere ($D_{eff}/D_a$) ranged from 0.1 to 0.5 across wells and through time, whereas the diffusion coefficient ratio for 20 cm depth varied by 100 times due to periods of water saturation alternating with drier periods at the midprofile depth. Therefore, the high $CO_2$ concentrations observed at deeper soil layers did not lead to high $CO_2$ production for those layers because they were largely a consequence of lower diffusivity, by 2 orders of magnitude, rather than higher $CO_2$ production.

### 4.3. Soil Profile $CO_2$ Flux and Soil $CO_2$ Production

[23] Soil profile $CO_2$ flux for the 0–10 cm layer ranged from 0.72 to 2.64 g $CO_2$-C $m^{-2}$ $d^{-1}$ across all 3 years'

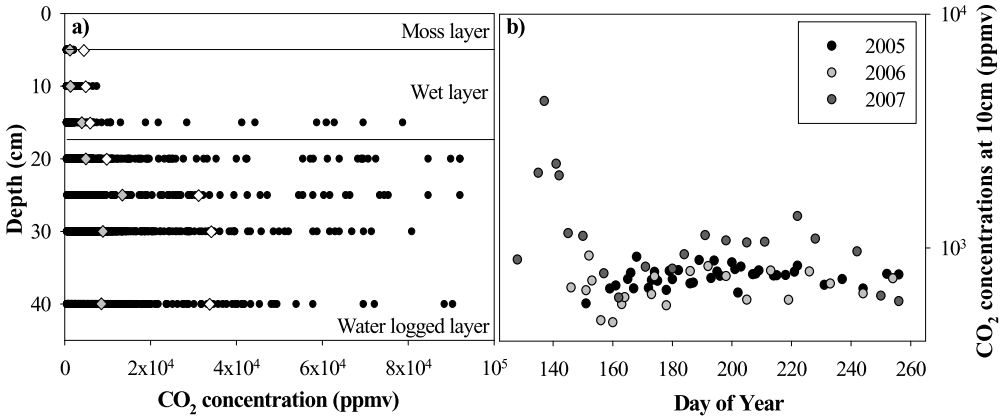


**Figure 1.** (a) Soil $CO_2$ concentrations sampled at 5 cm increments across three sites varying in degree of permafrost thaw from 2005 to 2007. The moss layer (0–5 cm) at the surface consists of live mosses. The wet layer (5–17.5 cm) below the moss is moist, and the moisture content varies seasonally with rainfall. The water-logged layer (>17.5 cm) is typically saturated with water for most of the growing season as a result of rain and meltwater perched on the ground ice. Mean values are shown with open diamonds, and median values are shown with gray diamonds for all soil $CO_2$ concentrations. (b) The seasonal trend of soil $CO_2$ concentration over the 3 year study. Each point represents an average value across all sites for a given sampling period. A single depth (10 cm) is shown for clarity; this depth reflects similar seasonal trends that occurred at all depths.

growing seasons, and $CO_2$ flux was highest at this depth among all soil layers observed (Figure 3). Even though $CO_2$ concentrations were high in the deepest soil layer (20–30 cm), $CO_2$ flux was low because the diffusion coefficient in this layer decreased due to water saturation. Mean soil $CO_2$ flux for the 20–30 cm layer ranged from 0 to $4.79 \times 10^{-4}$ g $CO_2$-C $m^{-2}$ $d^{-1}$ across all 3 years' growing seasons, but the error generated as a result of uncertain estimation of diffusion coefficient was $1.35 \times 10^{-5}$ g $CO_2$-C $m^{-2}$ $d^{-1}$. Therefore, even though we did not accurately estimate the diffusion coefficient at this depth, the error from poorly estimated diffusivity was very small due to low diffusion. As a result of decreasing diffusivity as the soil layer gets deeper, mean $CO_2$ flux in the 10–20 cm layer was only 10–20% that of the layer above, while mean $CO_2$ flux of 20–30 cm layer was 1–2 orders of magnitude smaller than that of 10–20 cm layer. When the mean $CO_2$ flux at 0–10 cm were compared by sites, Extensive Thaw was higher than Moderate and Minimal Thaw ($p < 0.001$ for both pairwise comparisons), but Moderate Thaw and Minimal Thaw were not significantly different from each other. This trend of the highest mean $CO_2$ flux being in the Extensive Thaw site was the same for the 10–20 cm ($p = 0.01$ for both pairwise comparisons) layer. In the deepest layer (20–30 cm), mean $CO_2$ flux at Extensive Thaw and Moderate Thaw was about 10% higher than Minimal Thaw; however, they were not statistically different from one another. Fluxes from soil deeper than 30 cm were not considered here, because those layers were either frozen or saturated during most of the growing season, and flux rates were very low.

[24] Aggregated across the growing season, the mean soil $CO_2$ production ranged from 0.96 to 2.52 g $CO_2$-C $m^{-2}$ $d^{-1}$, and was highest at Extensive Thaw and lowest at Minimal Thaw (Figure 4a). Mean soil $CO_2$ production at Extensive Thaw was significantly different from Moderate Thaw and Minimal Thaw ($p < 0.001$); however, Moderate Thaw was not different from Minimal Thaw. Site level soil temperature monitored at 10 cm depth showed (Figure 4b) that Extensive and Moderate Thaw were not different, but Minimal Thaw was significantly lower in 2005 and 2006 ($p < 0.001$). In 2007, Moderate Thaw was significantly higher than Extensive and Minimal Thaw ($p < 0.001$), but Extensive and Minimal Thaw were not different. Mean soil temperature at 10 cm in 2005 and 2006 were not different, but significantly lower in 2007 ($p < 0.001$). VWC at 10 cm in 2006 showed (Figure 4c) that Extensive and Moderate Thaw were not different, but Minimal Thaw was signifi-

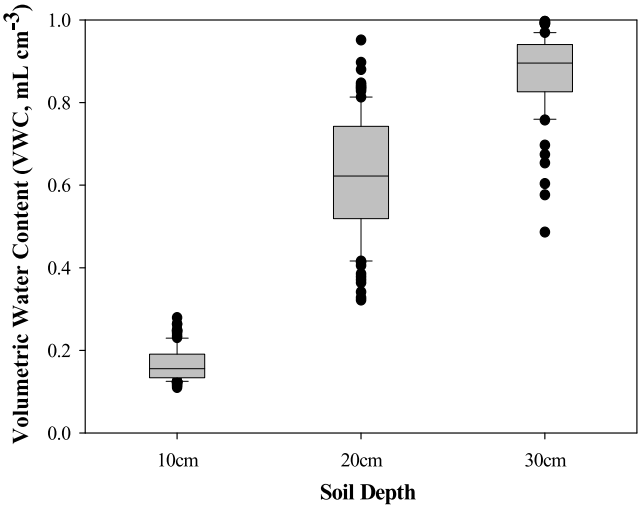


**Figure 2.** Box plot showing the distribution of volumetric water content (VWC). The plots show means with the 75th percentile within the box and the 95th percentile within the error bars. The VWC was measured in 2006 and 2007 during the growing season at all gas wells for 10, 20, and 30 cm depths when we sampled gas.

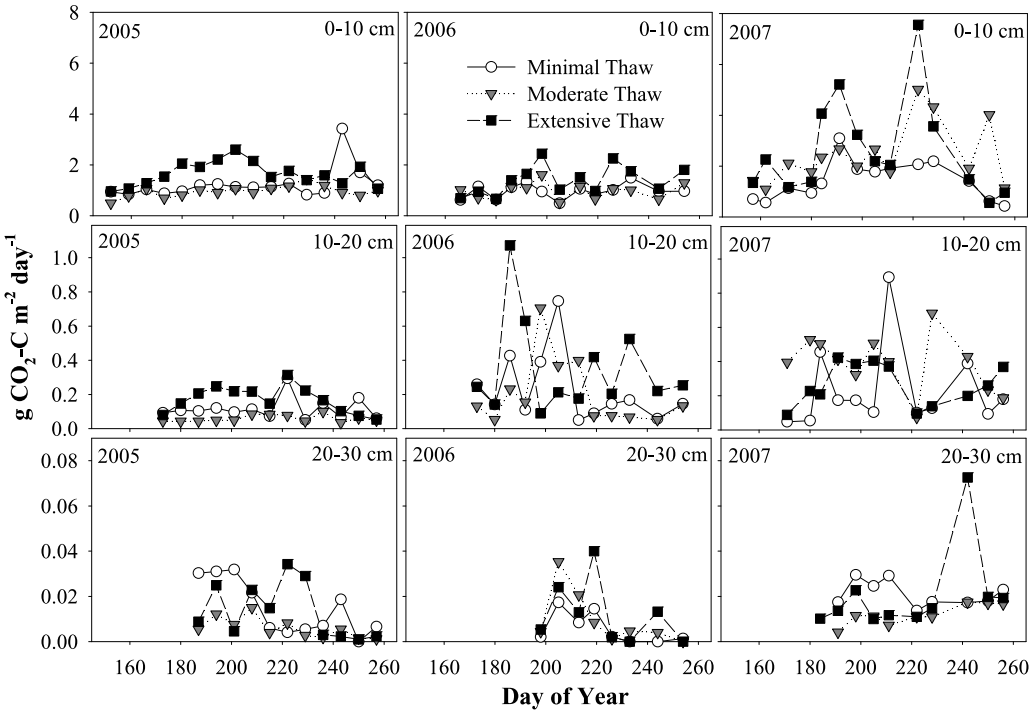


**Figure 3.** Soil profile $CO_2$ fluxes for the three sites during the growing season (June–August) from 2005 to 2007 calculated for 10 cm intervals. Each symbol of soil $CO_2$ fluxes represents a weekly mean averaged by site. Note the scale of the *y* axis changes for each different depth interval.

cantly lower ($p < 0.001$). VWC was different across the sites ($p < 0.001$) in 2007, highest in Extensive Thaw and lowest in Minimal Thaw, but we were not able to observe VWC in 2005. VWC at 10 cm in 2007 was significantly higher than 2006 ($p < 0.001$). Over the 3 years of observation, soil $CO_2$ production in 2007 was the highest and 2005 was the lowest, which may be due to higher frequency of rainfall, which was 145 mm in 2005 and 227 mm in 2006 from May to September [*Vogel et al.*, 2009], but was 285 in 2007 from 19 May to 19 September (J. Vogel, unpublished data, 2009). We speculate that increased precipitation level may have increased soil moisture especially at 5 and 10 cm in 2007 as a result. When soil $CO_2$ production was analyzed using repeated measures analysis, soil $CO_2$ production was different across the sites ($p = 0.02$) and years ($p < 0.001$). However, the site × year interaction was not different ($p = 0.23$), implying that the trend across sites was consistent throughout the 3 sampled years. When the mean soil $CO_2$ production was extrapolated to whole growing season $CO_2$ production (1 May to 31 September, 150 days), estimates of growing season $CO_2$ production from three sites were 270 g $CO_2$-C $m^{-2}$ at Extensive Thaw, 229 g $CO_2$-C $m^{-2}$ at Moderate Thaw, and 177 g $CO_2$-C $m^{-2}$ at Minimal Thaw. These estimates explained approximately 43–61% of total ecosystem respiration, when they were compared with surface $CO_2$ flux measurements from these sites [*Vogel et al.*, 2009].

### 4.4. Modeling Growing Season Soil $CO_2$ Production

[25] Pearson's partial correlations showed that Microtopography was negatively correlated with VWC (−0.5780), positively correlated with both dummy Site variables (Table 1), and only weakly correlated with ALT (0.0676). When all of the variables were used to model mean growing season soil $CO_2$ production, 54% of the variance in soil $CO_2$ production was explained in a full model (adjusted $R^2 = 0.38$). However, none of the parameters were significant at a $p = 0.10$ level in this model, except for Site 1 (the dummy variable for Extensive Thaw site), which implies that there is a multicoliniarity embedded within all of the parameters in the model. Variables "ALT" and "VWC" were not added to the regression model because adding those variables from "Sites+T+Microtopography" did not increase the $R^2$ of the model. Adjusted $R^2$ values account for increasing the number of variables. Variables were manually put in the model in addition to the single best variables ("Microtopography," "Sites") to maximize $R^2$ while maintaining significance for the rest of the variables. Therefore, we separated each variable in the multiple regression model to find the best predictor variable for soil $CO_2$ production. From this analysis, Microtopography was the best single predictor variable ($R^2 = 0.33$) for soil $CO_2$ production (Figure 5) followed by Sites 1 and 2 ($R^2 = 0.29$), and spatial variability of soil temperature at 10 cm ($R^2 = 0.15$) (Table 2). Spatial variability of soil temperature was positively correlated to soil $CO_2$ production, whereas Microtopography was negatively correlated to soil $CO_2$ production. This implies that increased soil temperature at microsite-scale increases soil $CO_2$ production, and soil $CO_2$ production was higher at the lower surfaces created by permafrost thaw and thermokarst development. Neither VWC nor ALT was significantly correlated to soil $CO_2$ production by themselves. When the Site variables were combined with Microtopography, the $R^2$ increased only 0.15, which implies that Site variables are not correlated to Microtopography. When we used Microtopography and T in the model, 41% of soil $CO_2$ production was explained by these

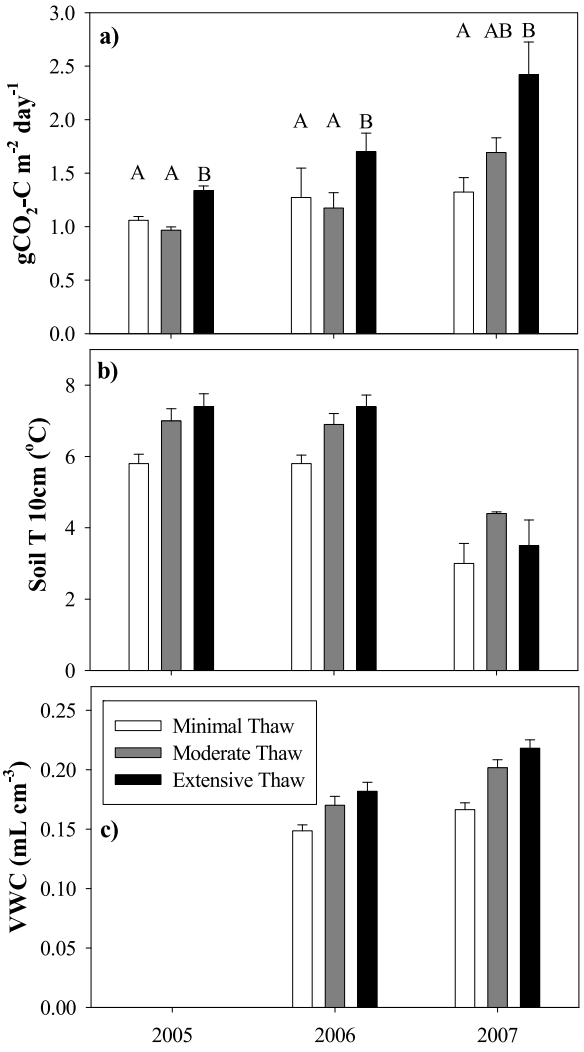


**Figure 4.** Mean (±SE) growing season (a) soil $CO_2$ production, (b) soil temperature at 10 cm, and (c) VWC at 10 cm by year. Different letters in Figure 4a represent significant differences in means between sites within a study year at $\alpha < 0.05$ using Tukey's paired test adjusted for multiple comparisons.

two variables (adjusted $R^2 = 0.36$). When Site variables were added to this model, $R^2$ increased up to 0.55, making it the best overall model for soil $CO_2$ production given the measured variables.

## 5. Discussion

[26] Soil profile $CO_2$ measurements provide detailed information on $CO_2$ production across the soil profile [*Davidson and Trumbore*, 1995]. We used this method to understand how permafrost thaw and thermokarst affects soil C emissions from different soil layers. Soil $CO_2$ production in this upland tundra sites showed both temporal and spatial variation; soil $CO_2$ production generally increased with increasing temperature during the growing season. More importantly, soil $CO_2$ production increased with the degree of permafrost thaw and thermokarst development across sites, likely as a result of changes in soil properties apart from seasonal variations in soil temperature. Higher total soil $CO_2$ production at Extensive Thaw (Figure 4a) was likely as a result of deeper permafrost thaw and more ground subsidence at this site. Soil $CO_2$ flux estimated for each 10 cm soil layer showed that the 0–10 cm surface layer contributed the most to the total soil $CO_2$ production, with the 10–20 cm layer having production an order of magnitude smaller in general (Figure 3). Even though deeper soil layers showed 100 times higher $CO_2$ concentrations (Figure 1) than the surface layer, soil $CO_2$ flux from these deeper layers was 2 orders of magnitude lower than surface soil $CO_2$ flux (Figure 3) due to low diffusivity in these water saturated soils.

[27] High correlations between microtopography and other environmental variables (Table 1) represent that surface subsidence may be a good predictor of changes in soil environment such as increased moisture and microsite surface soil temperatures corresponding to changes in microtopography. Among all the measured variables, soil moisture was correlated the highest with surface subsidence. When thermokarst develops, subsided areas are more likely to collect water and increase soil moisture content [*Jorgenson et al.*, 2006], while leaving other nearby areas drier. We observed that soil temperature in subsided areas was higher than in nearby less subsided areas [*Osterkamp et al.*, 2000; *Schuur et al.*, 2007]. One of the explanations that soil temperatures were higher in thermokarst depressions than in the surroundings is because subsided ground surfaces trap snow during winter as wind redistributes it across the landscape, which then further insulates soil during winter [*Osterkamp*, 2007a]. Warm winter soil positively feeds back to soil temperature during summer [*Stieglitz et al.*, 2003]. Correlations between site dummy variables and soil $CO_2$ production represent the effect of different sites in soil $CO_2$ production. These effects are independent of the measured variables (soil temperature, moisture, or ATL) but shows differences in the sites that may affect soil $CO_2$ production,

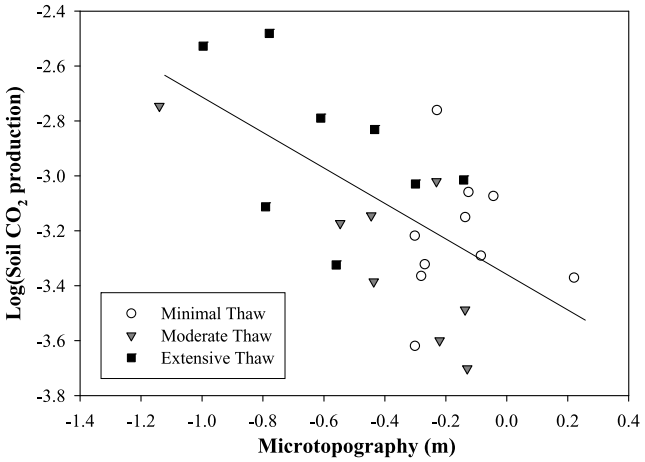


**Figure 5.** Relationship between relative microtopographic elevation of individual gas wells and soil $CO_2$ production. Microtopography was the best single predictor variable in the soil $CO_2$ production model ($R^2 = 0.33$, $p = 0.0021$, $y = -3.35 - 0.59x$). Symbols are mean values of log-transformed soil $CO_2$ production averaged from 2005 to 2007 for each gas well.

**Table 1.** Pearson's Pairwise Correlation Coefficients for the Environmental Variables Used in the Soil $CO_2$ Production Model[a]

| | Microtopography | T | VWC | ALT | Site 1 | Site 2 |
|---|---|---|---|---|---|---|
| Microtopography | | **−0.1059** | **−0.5752** | **−0.3442** | **0.4362** | **0.4835** |
| T | 0.4679 | | **0.1912** | **−0.0179** | **0.0288** | **0.0217** |
| VWC | 0.0014 | 0.3298 | | **0.0258** | **−0.2657** | **−0.3709** |
| ALT | 0.0675 | 0.9252 | 0.8965 | | **−0.1946** | **−0.3190** |
| Site1 | 0.0180 | 0.8798 | 0.1717 | 0.2859 | | **0.5000** |
| Site2 | 0.0079 | 0.9095 | 0.0520 | 0.0752 | 0.0030 | |

[a]Values in bold are correlation coefficients, and the rest of the values are p values. T, spatial variability in soil temperature at 10 cm; VWC, volumetric water content at 10 cm; ALT, active layer thickness. Sites 1 and 2 are dummy variables of sites represented by 0 and 1.

such as shifts in vegetation from tussock-forming sedges to shrub dominating tundra, or changes in total plant biomass [*Schuur et al.*, 2007]. The changes in the plant community could alter belowground $CO_2$ production independently of the observed environmental changes by increased root respiration, when there were no overall differences shown in soil C pools among sites. We suggest that surface subsidence created by permafrost thaw and thermokarst development in upland tundra may be a driver of changes in soil environment by redistributing water and snow that secondarily increase soil temperature and moisture that then affect the rate of soil organic matter decomposition and root respiration.

[28] A strong relationship between soil $CO_2$ production and microtopography, spatial variability in soil temperature, and sites (Table 2 and Figure 5) implies that surface subsidence induces change in soil properties that stimulates $CO_2$ emissions from root respiration and microbial decomposition of soil organic matter. Several field studies have shown relationships between ecosystem respiration and topography driven factors such as soil moisture, soil texture, and vegetation [*Epron et al.*, 2006; *Hanson et al.*, 1993; *Kang et al.*, 2003]. Soil $CO_2$ production increases with temperature because both root respiration and microbial decomposition of soil organic matter respond to the direct effect of temperature. Most studies observed increased soil respiration and ecosystem respiration as a result of increased air and soil temperature [*Davidson and Janssens*, 2006; *Davidson et al.*, 2000; *Fang and Moncrieff*, 2001], and several others observed a positive relationship between soil $CO_2$ emissions and soil moisture in tundra ecosystems [*Chapin et al.*, 1988; *Christensen et al.*, 1998; *Illeris et al.*, 2004; *Illeris and Jonasson*, 1999; *Oberbauer et al.*, 1992, 1991], suggesting that either plant or microbial respiration may be limited by soil moisture in tundra ecosystem. Even though Figure 4 shows that the mean soil $CO_2$ production at different years does not seem to correspond to site level growing season soil temperature, we still showed that the spatial variability of soil temperature was correlated to the mean soil $CO_2$ production (Table 2). This implies that soil $CO_2$ production is correlated to microsite level changes in soil environment at a microsite scale as well as site scale that are correlated to permafrost thaw and thermokarst development. Our results are consistent with both moisture and temperature having a positive effect on soil $CO_2$ production, with the main effect of microtopography acting to redistribute soil moisture. While thickening of the active layer may expose larger amount of soil organic matter to microbial decomposition [*Romanovsky et al.*, 1997]. We found that ALT was not significantly correlated to soil $CO_2$ production at these sites (Table 2), but ALT was correlated to microtopography and site 2 dummy variables. It is likely that ALT has an indirect effect on soil $CO_2$ production. We did not partition the contribution of root respiration and microbial respiration in this study, but several root trenching studies suggested that contribution of microbial respiration on belowground respiration ranges from 10 to 90% depending on the density vascular plants [*Hanson et al.*, 2000; *Ngao et al.*, 2007]. However, recent study conducted using radioactive carbon showed that the contribution of old carbon increased as a function of increased ecosystem respiration up to 40% [*Schuur et al.*, 2009]. Even though increased soil $CO_2$ production in our study was a result of both increased root respiration and microbial decomposition of soil organic matter, it is likely that the contribution of microbial decomposition of soil organic matter increased as a result of permafrost thaw and thermokarst development. Therefore, we suggest that surface subsidence created by permafrost thaw and thermokarst development stimulated soil organic matter decomposition

**Table 2.** Soil $CO_2$ Production Model Using Single and Multiple Variables[a]

| Model | $R^2$ | $R^2$ Adjusted | Model p | Microtopography | T |
|---|---|---|---|---|---|
| ALT | 0.00 | - | 0.9637 | - | - |
| VWC | 0.11 | - | 0.1062 | - | - |
| T | 0.15 | - | 0.0508 | - | - |
| Sites | 0.29 | - | 0.0189 | - | - |
| Microtopography | 0.33 | - | 0.0021 | - | - |
| T+Microtopography | 0.41 | 0.36 | 0.0022 | 0.0040 | 0.0898 |
| Sites+T | 0.42 | 0.34 | 0.0069 | - | 0.0401 |
| Sites+Microtopography | 0.48 | 0.41 | 0.0021 | 0.0097 | - |
| Sites+T+Microtopography | 0.55 | 0.46 | 0.0017 | 0.0241 | 0.0985 |

[a]Values in the "Model p" column represent the p values of the full model, and values in the "T" and "Microtopography" columns represent p values of each variable in the model.

and root respiration likely as a result of changes in soil properties such as increased soil temperature, moisture, and plant biomass.

[29] Soil profile $CO_2$ fluxes in the surface layers (both 0–10 cm and 10–20 cm) were different among sites, suggesting that permafrost thaw and thermokarst development stimulated $CO_2$ fluxes in these layers. In contrast, soil $CO_2$ flux from the deepest soil layers (20–30 cm, Figure 3) was not different among sites, suggesting that deeper soil organic matter decomposition was not stimulated as much as the surface soil layers as a result of permafrost thaw and thermokarst development. This was contrary to the original hypothesis that deeper soil layers may contribute more to soil $CO_2$ production following permafrost thaw. Even though $CO_2$ concentrations collected from deeper depths (30 and 40 cm) gas samples were, on average, 10 times higher than at 10 cm depth, the deepest soil layer contributed less than 10% to soil $CO_2$ production; high concentrations were due to low diffusivity, which was 1/100 that of the diffusivity in the surface layers. A previous study conducted at the EML gradient sites observed that ALT at Extensive and Moderate Thaw sites were greater than Minimal Thaw. The two sites with increased thermokarst development showed extended ALT down to a meter as well as increased soil temperatures at 30 and 40 cm [*Vogel et al.*, 2009]. However, water saturation throughout the growing season in many subsided places may have prevented faster decomposition of soil organic matter. Therefore, water saturation in the deepest thawed areas may have offset the effect of higher temperature where the most ground subsidence occurred.

[30] Finally, we observed high $CO_2$ concentrations early in the growing season (Figure 1b) that do not agree with normal $CO_2$ temperature response curves, because soil temperatures are still quite low at this time of year and the seasonal thaw depth was shallow. We were not able to estimate the size and distribution of these air pockets. When we sampled gas, 20 mL of gas samples were drawn each time before the soil thawed and the $CO_2$ concentrations increased over time until the soil thawed. We speculate that these observations may be caused by physical storage and release of fall gas trap and winter respiration [*Monson et al.*, 2006; *Schimel et al.*, 2006] within frozen soils due to limited diffusion through ice layers [*Albert and Perron*, 2000], rather than a stimulation of biological $CO_2$ production during spring thaw. It is also likely that the soil gas present in the fall before freezing was trapped in the air pockets as the soil freezes from the surface. In the fall, the active layer freezes from the permafrost surface as well as soil surface due to sudden drop in air temperature. The trapped $CO_2$ concentrations may increase when microbial respiration continuously gets trapped during the winter. Pulses of high surface $CO_2$ flux during early spring have been observed [*Elberling and Brandt*, 2003; *Grogan et al.*, 2004] as well as sporadic pulses during the winter in a tundra flux study [*Friborg et al.*, 2008], which may be from release of trapped $CO_2$ in these air pockets when there are sudden cracks in frozen soil or when soil starts to thaw in spring. High $CO_2$ concentrations in gas wells within the frozen soil suggest a different interpretation for winter and early spring soil $CO_2$ concentrations beyond the normal flux diffusion model. Assuming the diffusion was near zero for these trapped air pockets, we estimated the winter soil $CO_2$ storage in pore spaces within frozen soils to better understand the potential magnitude of this C storage. To estimate potential soil $CO_2$ storage, we first assumed that the air volume in frozen soils was similar to air-filled porosity in unfrozen soil (measured during the growing season) to be conservative, and that the sampled $CO_2$ concentrations in the early spring represented the storage of $CO_2$ during winter. Using sampled $CO_2$ concentrations, estimated pore-space volume, and the ideal gas law, we calculate that this winter soil $CO_2$ storage could be between 0.01 g $CO_2$-C $m^{-2}$ and 1.48 g $CO_2$-C $m^{-2}$ for a given 10 cm layer of soil. This likely represents a maximum estimate because it assumes that the trapped air pocket is continuous for a given layer. Recent studies observed winter $CO_2$ fluxes from 20 to 75 g $CO_2$-C $m^{-2}$, and emphasized the importance of winter respiration that had been neglected in the high-latitude ecosystems [*Kim et al.*, 2007; *Oechel et al.*, 2000; *Sullivan et al.*, 2008]. However, the studies using base traps showed wider range of winter $CO_2$ fluxes, such as 1 to 190 g $CO_2$-C $m^{-2}$ [*Grogan and Chapin*, 1999; *Welker et al.*, 2000]. Our estimates are small compared to $CO_2$ fluxes from annual respiration, which is on the range of 300–400 g $CO_2$-C $m^{-2}$ from these sites, with winter respiration ranging from 48 to 104 g $CO_2$-C $m^{-2}$ [*Vogel et al.*, 2009]. However, our estimate of winter soil $CO_2$ storage is simply an estimate of $CO_2$ storage in the small ice cavity in frozen soil, not the $CO_2$ fluxes throughout the long winter season in tundra ecosystem. We suggest that $CO_2$ stored in the ice cavity may be part of a $CO_2$ source that needs to be accounted in annual carbon balance estimates.

## 6. Conclusion

[31] In summary, we supported the projection that permafrost thaw and thermokarst development will increase permafrost carbon emissions by stimulating soil organic matter decomposition and root respiration. This stimulation results from increased soil temperature, moisture, and thickening of the active layer associated with surface subsidence created by permafrost thaw and thermokarst development. Ground surface subsidence created by permafrost thaw and thermokarst development was the best predictor of soil $CO_2$ production but was also correlated to other environmental variables such as soil moisture, indicating that ground subsidence induces changes in soil properties and can be used as an integrated metric for other environmental variables. Our results showed that the surface layer was the most affected by thaw. We also observed unusually high $CO_2$ concentrations in the early growing season, which may be trapped $CO_2$ within air pockets in the frozen soil; a result of soil surface freeze in the fall and restricted diffusion of $CO_2$ produced during winter respiration. Although here we do not show the direct effect of soil organic matter decomposition on increased soil $CO_2$ production, increased soil organic matter decomposition was indeed a major source of soil $CO_2$ production at this site as shown with isotope source partitioning measurements [*Schuur et al.*, 2009]. Future measurements of soil methane production and fluxes from different soil depths would be useful for estimating overall climate forcing of greenhouse gas emissions from permafrost thaw in high-latitude ecosystems.

[32] **Acknowledgments.** This research was funded in part by multiple grants to E.A.G.S.: NSF DEB-0516326; the LTER program (DEB-0080609, DEB-0423442, DEB-0620579); and NASA New Investigator Program grant. GPS units were facilitated by UNAVCO. We would like to acknowledge George Casella and Statistical Consulting Program at the Department of Statistics, University of Florida, for discussion on statistical analysis and model construction. We thank A. Baron, A. Frisbee, M. Goldschlag, L. Gutierrez, and C. Trucco for help on field work.

## References

Albert, M. R., and F. E. Perron (2000), Ice layer and surface crust permeability in a seasonal snow pack, *Hydrol. Process.*, *14*(18), 3207–3214, doi:10.1002/1099-1085(20001230)14:18<3207::AID-HYP196>3.0.CO;2-C.

Arctic Climate Impact Assessment (ACIA) (2005), *Arctic Climate Impact Assessment—Scientific Report*, Cambridge Univ. Press, New York.

Chapin, F. S., N. Fetcher, K. Kielland, K. R. Everett, and A. E. Linkins (1988), Productivity and nutrient cycling of Alaskan tundra—Enhancement by flowing soil-water, *Ecology*, *69*(3), 693–702, doi:10.2307/1941017.

Christensen, T. R., S. Jonasson, A. Michelsen, T. V. Callaghan, and M. Havstrom (1998), Environmental controls on soil respiration in the Eurasian and Greenlandic Arctic, *J. Geophys. Res.*, *103*(D22), 29,015–29,021, doi:10.1029/98JD00084.

Davidson, E. A., and I. A. Janssens (2006), Temperature sensitivity of soil carbon decomposition and feedbacks to climate change, *Nature*, *440*(7081), 165–173, doi:10.1038/nature04514.

Davidson, E. A., and S. E. Trumbore (1995), Gas diffusivity and production of $CO_2$ in deep soils of the eastern Amazon, *Tellus, Ser. B*, *47*(5), 550–565, doi:10.1034/j.1600-0889.47.issue5.3.x.

Davidson, E. A., L. V. Verchot, J. H. Cattanio, I. L. Ackerman, and J. E. M. Carvalho (2000), Effects of soil water content on soil respiration in forests and cattle pastures of eastern Amazonia, *Biogeochemistry*, *48*(1), 53–69, doi:10.1023/A:1006204113917.

Elberling, B., and K. K. Brandt (2003), Uncoupling of microbial $CO_2$ production and release in frozen soil and its implications for field studies of arctic C cycling, *Soil Biol. Biochem.*, *35*(2), 263–272, doi:10.1016/S0038-0717(02)00258-4.

Elberling, B., and P. Ladegaard-Pedersen (2005), Subsurface $CO_2$ dynamics in temperate beech and spruce forest stands, *Biogeochemistry*, *75*(3), 479–506, doi:10.1007/s10533-005-3690-9.

Epron, D., A. Bosc, D. Bonal, and V. Freycon (2006), Spatial variation of soil respiration across a topographic gradient in a tropical rain forest in French Guiana, *J. Trop. Ecol.*, *22*, 565–574, doi:10.1017/S0266467406003415.

Fang, C., and J. B. Moncrieff (2001), The dependence of soil $CO_2$ efflux on temperature, *Soil Biol. Biochem.*, *33*(2), 155–165, doi:10.1016/S0038-0717(00)00125-5.

Fortier, D., M. Allard, and Y. Shur (2007), Observation of rapid drainage system development by thermal erosion of ice wedges on Bylot island, Canadian Arctic Archipelago, *Permafrost Periglac. Processes*, *18*(3), 229–243, doi:10.1002/ppp.595.

Friborg, T., B. Elberling, B. U. Hansen, L. A. Jensen, L. B. Smith, J. Soendergaard, and M. Mastepanov (2008), Winter time burst of $CO_2$ from the high arctic soils of Svalbard, *Eos Trans. AGU*, *89*(53), Fall Meet. Suppl., Abstract B11A–0325.

Gaudinski, J. B., S. E. Trumbore, E. A. Davidson, and S. H. Zheng (2000), Soil carbon cycling in a temperate forest: Radiocarbon-based estimates of residence times, sequestration rates and partitioning of fluxes, *Biogeochemistry*, *51*(1), 33–69, doi:10.1023/A:1006301010014.

Grogan, P., and F. S. Chapin (1999), Arctic soil respiration: Effects of climate and vegetation depend on season, *Ecosystems*, *2*(5), 451–459, doi:10.1007/s100219900093.

Grogan, P., A. Michelsen, P. Ambus, and S. Jonasson (2004), Freeze-thaw regime effects on carbon and nitrogen dynamics in sub-arctic heath tundra mesocosms, *Soil Biol. Biochem.*, *36*(4), 641–654, doi:10.1016/j.soilbio.2003.12.007.

Hanson, P. J., S. D. Wullschleger, S. A. Bohlman, and D. E. Todd (1993), Seasonal and topographic patterns of forest floor $CO_2$ efflux from an upland oak forest, *Tree Physiol.*, *13*(1), 1–15.

Hanson, P. J., N. T. Edwards, C. T. Garten, and J. A. Andrews (2000), Separating root and soil microbial contributions to soil respiration: A review of methods and observations, *Biogeochemistry*, *48*(1), 115–146, doi:10.1023/A:1006244819642.

Hirsch, A. I., S. E. Trumbore, and M. L. Goulden (2002), Direct measurement of the deep soil respiration accompanying seasonal thawing of a boreal forest soil, *J. Geophys. Res.*, *107*, 8221, doi:10.1029/2001JD000921 [printed *108*(D23), 2003].

Hirsch, A. I., S. E. Trumbore, and M. L. Goulden (2004), The surface $CO_2$ gradient and pore-space storage flux in a high-porosity litter layer, *Tellus, Ser. B*, *56*(4), 312–321, doi:10.1111/j.1600-0889.2004.00113.x.

Illeris, L., and S. Jonasson (1999), Soil and plant $CO_2$ emission in response to variations in soil moisture and temperature and to amendment with nitrogen, phosphorus, and carbon in northern Scandinavia, *Arct. Antarct. Alp. Res.*, *31*(3), 264–271, doi:10.2307/1552256.

Illeris, L., T. R. Christensen, and M. Mastepanov (2004), Moisture effects on temperature sensitivity of $CO_2$ exchange in a subarctic heath ecosystem, *Biogeochemistry*, *70*(3), 315–330, doi:10.1007/s10533-003-0855-2.

Jahne, B., G. Heinz, and W. Dietrich (1987), Measurement of the diffusion-coefficients of sparingly soluble gases in water, *J. Geophys. Res.*, *92*(C10), 10,767–10,776, doi:10.1029/JC092iC10p10767.

Jorgenson, M. T., C. H. Racine, J. C. Walters, and T. E. Osterkamp (2001), Permafrost degradation and ecological changes associated with a warming climate in central Alaska, *Clim. Change*, *48*(4), 551–579, doi:10.1023/A:1005667424292.

Jorgenson, M. T., Y. L. Shur, and E. R. Pullman (2006), Abrupt increase in permafrost degradation in Arctic Alaska, *Geophys. Res. Lett.*, *33*, L02503, doi:10.1029/2005GL024960.

Kang, S. Y., S. Doh, D. Lee, V. L. Jin, and J. S. Kimball (2003), Topographic and climatic controls on soil respiration in six temperate mixed-hardwood forest slopes, Korea, *Global Change Biol.*, *9*(10), 1427–1437, doi:10.1046/j.1365-2486.2003.00668.x.

Kim, Y., M. Ueyama, F. Nakagawa, U. Tsunogai, Y. Harazono, and N. Tanaka (2007), Assessment of winter fluxes of $CO_2$ and $CH_4$ in boreal forest soils of central Alaska estimated by the profile method and the chamber method: A diagnosis of methane emission and implications for the regional carbon budget, *Tellus, Ser. B*, *59*(2), 223–233, doi:10.1111/j.1600-0889.2006.00233.x.

Lee, H., E. A. G. Schuur, and J. G. Vogel (2007), Spatial variation in carbon release from arctic tundra resulting from microtopography created by permafrost thawing, *Eos Trans. AGU*, *88*(52), Fall Meet. Suppl., Abstract B23D–1602.

Little, J. D., H. Sandall, M. T. Walegur, and F. E. Nelson (2003), Application of Differential Global Positioning Systems to monitor frost heave and thaw settlement in tundra environments, *Permafrost Periglac. Processes*, *14*(4), 349–357, doi:10.1002/ppp.466.

Millington, R. J. (1959), Gas diffusion in porous media, *Science*, *130*(3367), 100–102, doi:10.1126/science.130.3367.100-a.

Monson, R. K., D. L. Lipson, S. P. Burns, A. A. Turnipseed, A. C. Delany, M. W. Williams, and S. K. Schmidt (2006), Winter forest soil respiration controlled by climate and microbial community composition, *Nature*, *439*(7077), 711–714, doi:10.1038/nature04555.

Ngao, J., B. Longdoz, A. Granier, and D. Epron (2007), Estimation of autotrophic and heterotrophic components of soil respiration by trenching is sensitive to corrections for root decomposition and changes in soil water content, *Plant Soil*, *301*(1–2), 99–110, doi:10.1007/s11104-007-9425-z.

Oberbauer, S. F., J. D. Tenhunen, and J. F. Reynolds (1991), Environmental-effects on $CO_2$ efflux from water track and tussock tundra in Arctic Alaska, USA, *Arct. Alp. Res.*, *23*(2), 162–169, doi:10.2307/1551380.

Oberbauer, S. F., C. T. Gillespie, W. Cheng, R. Gebauer, A. S. Serra, and J. D. Tenhunen (1992), Environmental-effects on $CO_2$ efflux from riparian tundra in the northern foothills of the Brooks Range, Alaska, USA, *Oecologia*, *92*(4), 568–577, doi:10.1007/BF00317851.

Oechel, W. C., G. L. Vourlitis, S. J. Hastings, R. C. Zulueta, L. Hinzman, and D. Kane (2000), Acclimation of ecosystem $CO_2$ exchange in the Alaskan Arctic in response to decadal climate warming, *Nature*, *406*(6799), 978–981, doi:10.1038/35023137.

Oh, N. H., H. S. Kim, and D. D. Richter (2005), What regulates soil $CO_2$ concentrations?—A modeling approach to $CO_2$ diffusion in deep soil profiles, *Environ. Eng. Sci.*, *22*(1), 38–45, doi:10.1089/ees.2005.22.38.

Osterkamp, T. E. (2005), The recent warming of permafrost in Alaska, *Global Planet. Change*, *49*(3–4), 187–202, doi:10.1016/j.gloplacha.2005.09.001.

Osterkamp, T. E. (2007a), Causes of warming and thawing permafrost in Alaska, *Eos Trans. AGU*, *88*(48), 522, doi:10.1029/2007EO480002.

Osterkamp, T. E. (2007b), Characteristics of the recent warming of permafrost in Alaska, *J. Geophys. Res.*, *112*, F02S02, doi:10.1029/2006JF000578.

Osterkamp, T. E., and V. E. Romanovsky (1999), Evidence for warming and thawing of discontinuous permafrost in Alaska, *Permafrost Periglac. Processes*, *10*(1), 17–37, doi:10.1002/(SICI)1099-1530(199901/03)10:1<17::AID-PPP303>3.0.CO;2-4.

Osterkamp, T. E., L. Viereck, Y. Shur, M. T. Jorgenson, C. Racine, A. Doyle, and R. D. Boone (2000), Observations of thermokarst and its impact on boreal forests in Alaska, USA, *Arct. Antarct. Alp. Res.*, *32*(3), 303–315, doi:10.2307/1552529.

Risk, D., L. Kellman, and H. Beltrami (2002), Soil $CO_2$ production and surface flux at four climate observatories in eastern Canada, *Global Biogeochem. Cycles*, *16*(4), 1122, doi:10.1029/2001GB001831.

Romanovsky, V. E., T. E. Osterkamp, and N. S. Duxbury (1997), An evaluation of three numerical models used in simulations of the active layer and permafrost temperature regimes, *Cold Reg. Sci. Technol.*, *26*(3), 195–203, doi:10.1016/S0165-232X(97)00016-5.

Schimel, J. P., J. Fahnestock, G. Michaelson, C. Mikan, C. L. Ping, V. E. Romanovsky, and J. Welker (2006), Cold-season production of $CO_2$ in arctic soils: Can laboratory and field estimates be reconciled through a simple modeling approach?, *Arct. Antarct. Alp. Res.*, *38*(2), 249–256, doi:10.1657/1523-0430(2006)38[249:CPOCIA]2.0.CO;2.

Schuur, E. A. G., K. G. Crummer, J. G. Vogel, and M. C. Mack (2007), Plant species composition and productivity following permafrost thaw and thermokarst in Alaskan tundra, *Ecosystems*, *10*(2), 280–292, doi:10.1007/s10021-007-9024-0.

Schuur, E. A. G., et al. (2008), Vulnerability of permafrost carbon to climate change: Implications for the global carbon cycle, *BioScience*, *58*(8), 701–714, doi:10.1641/B580807.

Schuur, E. A. G., J. G. Vogel, K. G. Crummer, H. Lee, J. O. Sickman, and T. E. Osterkamp (2009), The impact of permafrost thaw on old carbon release and net carbon exchange from tundra, *Nature*, *459*, 556–559, doi:10.1038/nature08031.

Serreze, M. C., J. E. Walsh, F. S. Chapin, T. Osterkamp, M. Dyurgerov, V. Romanovsky, W. C. Oechel, J. Morison, T. Zhang, and R. G. Barry (2000), Observational evidence of recent change in the northern high-latitude environment, *Clim. Change*, *46*(1–2), 159–207, doi:10.1023/A:1005504031923.

Shaver, G. R., L. C. Johnson, D. H. Cades, G. Murray, J. A. Laundre, E. B. Rastetter, K. J. Nadelhoffer, and A. E. Giblin (1998), Biomass and $CO_2$ flux in wet sedge tundras: Responses to nutrients, temperature, and light, *Ecol. Monogr.*, *68*(1), 75–97.

Stieglitz, M., S. J. Dery, V. E. Romanovsky, and T. E. Osterkamp (2003), The role of snow cover in the warming of arctic permafrost, *Geophys. Res. Lett.*, *30*(13), 1721, doi:10.1029/2003GL017337.

Sullivan, P. F., J. M. Welker, S. J. T. Arens, and B. Sveinbjornsson (2008), Continuous estimates of $CO_2$ efflux from arctic and boreal soils during the snow-covered season in Alaska, *J. Geophys. Res.*, *113*, G04009, doi:10.1029/2008JG000715.

Takahashi, A., T. Hiyama, H. A. Takahashi, and Y. Fukushima (2004), Analytical estimation of the vertical distribution of $CO_2$ production within soil: Application to a Japanese temperate forest, *Agric. For. Meteorol.*, *126*(3–4), 223–235, doi:10.1016/j.agrformet.2004.06.009.

Tang, J. W., D. D. Baldocchi, Y. Qi, and L. K. Xu (2003), Assessing soil $CO_2$ efflux using continuous measurements of $CO_2$ profiles in soils with small solid-state sensors, *Agric. For. Meteorol.*, *118*(3–4), 207–220, doi:10.1016/S0168-1923(03)00112-6.

Tarnocai, C., J. Canadell, G. Mazhitova, E. A. G. Schuur, P. Kuhry, and S. Zimov (2009), Soil organic carbon stocks in the northern circumpolar permafrost region, *Global Biogeochem. Cycles*, *23*, GB2023, doi:10.1029/2008GB003327.

Vogel, J., E. A. G. Schuur, C. Trucco, and H. Lee (2009), Response of $CO_2$ exchange in a tussock tundra ecosystem to permafrost thaw and thermokarst development, *J. Geophys. Res.*, *114*, G04018, doi:10.1029/2008JG000901.

Vourlitis, G. L., and W. C. Oechel (1999), Eddy covariance measurements of $CO_2$ and energy fluxes of an Alaskan tussock tundra ecosystem, *Ecology*, *80*(2), 686–701, doi:10.1890/0012-9658(1999)080[0686:ECMOCA]2.0.CO;2.

Welker, J. M., J. T. Fahnestock, and M. H. Jones (2000), Annual $CO_2$ flux in dry and moist arctic tundra: Field responses to increases in summer temperatures and winter snow depth, *Clim. Change*, *44*(1–2), 139–150, doi:10.1023/A:1005555012742.

H. Lee, Department of Biology, New Mexico State University, Las Cruces, NM 88003, USA. (hlee@nmsu.edu)

E. A. G. Schuur, Department of Biology, University of Florida, Gainesville, FL 32611, USA.

J. G. Vogel, School of Forest Resources and Conservation, University of Florida, Gainesville, FL 32611, USA.